Magnetocaloric effect across the coupled structural and ferromagnetic transition in $Pr_{0.1}Ce_{0.4}Sr_{0.5}MnO_3$[†]

C MADHU and A SUNDARESAN*

Chemistry and Physics of Materials Unit, Jawaharlal Nehru Center for Advanced Scientific Research, Jakkur Post, Bangalore 560 064
e-mail: sundaresan@jncasr.ac.in

Abstract. We have investigated the magnetocaloric effect across a first order structural transition coupled to the ferromagnetic transition ($T_C \sim 270$ K) in $Pr_{0.1}Ce_{0.4}Sr_{0.5}MnO_3$ using magnetization and heat capacity measurements. The adiabatic magnetic entropy change $|\Delta S|$ obtained from magnetization measurements for a magnetic field change of 2 T is around 1·3 J/kg K. A similar value of $|\Delta S|$ was obtained from the analysis of heat capacity data.

Keywords. Magnetocaloric effect; heat capacity; manganates; ferromagnetism.

1. Introduction

Recently, there has been a great deal of interest in magnetic materials showing large magnetocaloric effect (MCE). MCE is change in temperature of a magnetic material in adiabatic condition as a result of the alignment of its magnetic spins on exposure to an external magnetic field, the phenomenon which forms the basis for magnetic refrigeration. A large magnetocaloric effect was reported near room temperature in Gd and its alloys because of their large magnetic moment and magnetic entropy.[1–4] It is interesting to note a giant MCE in $Gd_5(Ge_{1-x}Si_x)_4$ where the coupled first-order structural transition and ferromagnetic transition gives a large magnetic entropy. In some materials, a first-order paramagnetic–ferromagnetic transition has strong influence on the MCE.[5,6] Very recently, perovskite manganese oxides which are known for their colossal magnetoresistance property have been shown to exhibit large MCE.[7–15] They exhibit not only large magnetic entropy, large heat capacities, but also their magnetic transition temperature can be tuned over a wide range of temperature. A large magnetic entropy has been observed at the charge-ordered antiferromagnetic transition for example, in $R_{0.5}Sr_{0.5}MnO_3$ (where R = Pr, Nd). In these materials, it is well known that the applied field destroys the charge-ordered state which is accompanied by structural and magnetic transitions.[7,12]

The material $Pr_{0.1}Ce_{0.4}Sr_{0.5}MnO_3$, has been reported to be ferromagnetic with the transition temperature ~ 270 K. It has an orthorhombic structure (space group Imma) at room temperature. From the neutron diffraction measurements, a small amount of secondary phase (about 5%) with similar composition was also found to be present in the sample. The secondary phase was reported to be tetragonal with the space group I4/mcm.[16,17] With decrease of temperature, the Imma phase transforms to I4/mcm at about 270 K, which was accompanied by the ferromagnetic transition. However, a complete structural phase transition was observed only at 210 K. At 270 K and 250 K, the amount of tetragonal phase was 12% and 18% respectively. Below 210 K, the structure remains tetragonal down to 1·5 K. The structural transition between the orthorhombic and tetragonal phase was found to be first-order. The coupled structural and ferromagnetic transitions may influence the MCE. In order to examine this idea, we have studied the MCE in the material $Pr_{0.1}Ce_{0.4}Sr_{0.5}MnO_3$.

2. Experimental

Polycrystalline sample, $Pr_{0.1}Ce_{0.4}Sr_{0.5}MnO_3$, was prepared by the conventional solid state reaction method. Stoichiometric proportion of the starting materials Mn_2O_3 (99% Aldrich), $SrCO_3$ (99·9% Aldrich), CeO_2 (99·995% Aldrich), Pr_6O_{11} (99·9% Alfa Aesar) were mixed thoroughly and the mixture was heated at 900°C, 1200°C, 1300°C and 1400°C for 12 h with intermediate grinding. The final sintering

was done at 1475°C. Phase purity was checked using powder X-ray diffraction (XRD) data. Magnetization measurements were performed using Vibrating Sample Magnetometer on Physical Property Measuring System (PPMS) of Quantum Design, USA. For measuring the magnetization (M) versus temperature (T) curve, sample was warmed slowly, stabilized at the desired temperature, and M was measured. The heat capacity measurement was performed with PPMS using Heat Capacity Option, which is based on thermal relaxation of the sample.

3. Results and discussion

The XRD pattern showed that the structure is orthorhombic as reported earlier.[16] The presence of secondary phase of a similar composition could not be confirmed by the XRD. However, we believe that the presence of such a small amount of tetragonal phase may not influence the results significantly. The magnetization versus temperature curves, under different applied field conditions, for $Pr_{0.1}Ce_{0.4}Sr_{0.5}MnO_3$ is shown in figure 1. The ferromagnetic transition temperature obtained from magnetization data measured at 0·005 T is around 270 K as seen in the inset of figure 1. Magnetization curves shown in figure 1 were obtained by first cooling the sample in presence of magnetic field to 160 K and then warming the sample to 320 K in step of 2 K. At each temperature the sample was stabilized for 30 s before the data were collected.
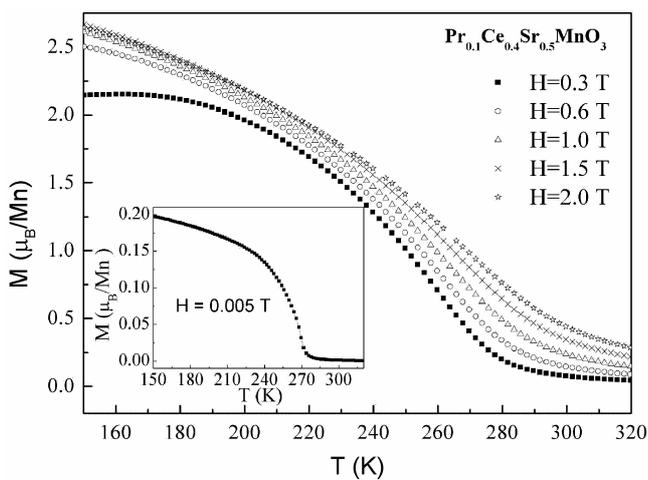
Figure 2 shows the magnetization as a function of magnetic field at different temperatures around T_C. In inset we have plotted the Arrott plot that confirms the magnetic transition to be from paramagnetic ($\varepsilon < 0$) to ferromagnetic ($\varepsilon > 0$) and also the T_C obtained from this plot, where $\varepsilon = 0$, is 265 K.[18,19]

We employ indirect method to calculate MCE as described in earlier reports (Neumeier *et al*[8]; Dinesen *et al*[9]). The origin of the magnetocaloric effect is due to coupling of magnetic sub-lattice with the magnetic field, which results in magnetic entropy
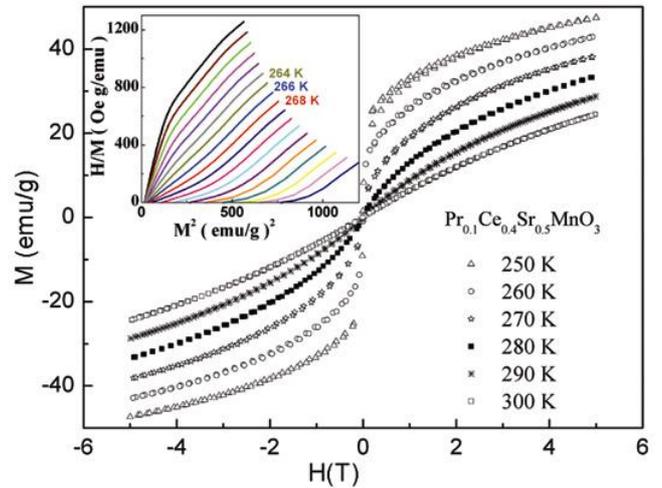

Figure 2. *M* versus *H* curve measured at different temperatures across the magnetic transition region. Inset is Arrott plot from 258 K to 276 K at step of 2 K.

Figure 1. Magnetization versus temperature curves, in presence of applied field of 0·3 T, 0·6 T, 1 T, 1·5 T and 2 T. Inset displays the sharp magnetic transition observed in presence of 0·005 T.
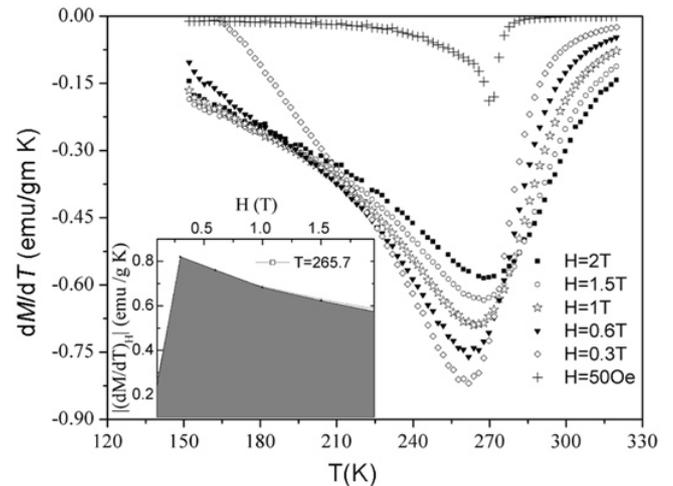

Figure 3. The derivatives of magnetization with respect to temperature, $(\partial M/\partial T)_H$ data at different applied fields are displayed. Inset shows $|(\partial M/\partial T)_H|$ versus *H* plot at 265·7 K. The shaded area under the curve corresponds to the $|\Delta S|$ value.

change (ΔS) which in turn gives rise to change in temperature (ΔT_{ad}) under adiabatic condition. These two thermodynamic quantities depend on temperature and are measured on the magnetic field. Thus, the magnetocaloric effect can be evaluated by measuring the magnetization and heat capacity with the use of the theory of thermodynamics. The Maxwell relation (1) relates the entropy change and magnetization,

$$\left(\frac{\partial M}{\partial T}\right)_H = \left(\frac{\partial S}{\partial H}\right)_T, \tag{1}$$

where M is the magnetization, T is the temperature, S is the magnetic entropy and H is the magnetic field. On integrating the above equation over the field range we get,

$$\Delta S = \int_0^{H_{max}} \left(\frac{\partial M}{\partial T}\right)_H dH, \tag{2}$$

which can be used to obtain the change in the magnetic entropy. The total entropy $|\Delta S|$, is determined by taking the derivative of magnetization data and find the area under the $(\partial M/\partial T)_H$ versus H curve. From (2), it is evident that this approximates the area under the $(\partial M/\partial T)_H$ versus H curve as rectangle. To find the maximum in $|\Delta S|$ more precisely, derivatives at number of magnetic fields, 0.005 T, 0.3 T, 0.6 T, 1 T, 1.5 T and 2 T were determined as shown in figure 3. The obtained values of $|\Delta S|$ are plotted as a function of temperature as shown in figure 4 for an applied field of 2 T. It is obvious from this figure
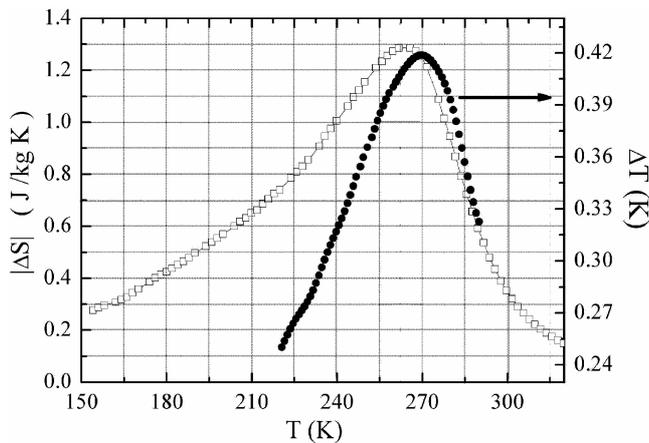
that there is peak in $|\Delta S|$ which is defined as $|\Delta S|_{max}$. It is interesting to note that the $|\Delta S|_{max}$ occurs near the ferromagnetic transition temperature T_C.

Increasing magnetic field shifts T_C to higher temperature but broadens the $M(T)$ curve due to fluctuation effects.[8] Further, it shifts the maximum in $(\partial M/\partial T)_H$ to higher temperature and reduce the value of $|\Delta S|_{max}$. The value of $|\Delta S|_{max}$ obtained for a magnetic field change of 2 T is about 1.3 J/kg K which is moderate. In contrast to the large magnetic entropy observed in many materials where there is a first-order structural transition near the magnetic transition, the present system shows relatively lower value of magnetic entropy. This may be due to lack of complete structural phase transition near the ferromagnetic transition as discussed in the introduction.

Although measurements of $|\Delta S|_{max}$ from magnetization data provide a good guide to the magnitude of magnetocaloric effect, it is essential that heat capacity measurements be used as well to make a complete evolution of MCE. Heat capacity data collected at zero and 2 T field in the temperature range 220–300 K are plotted in the inset of figure 5. These data were used to determine $|\Delta S|$ and compare its value to the one obtained from magnetization data.

The magnetocaloric effect is the change in temperature $\Delta T = [T(H) - T(0)]$ of magnetic material in the adiabatic condition with the application of the external magnetic field.[13] This effect originates due to the change of magnetic entropy of magnetic material in the presence of magnetic field. For ferromag-

Figure 4. The value of $|\Delta S|$ versus temperature calculated from magnetization data (in open circle). The change in temperature ΔT versus T calculated from heat capacity data using equation 4 (closed circle).
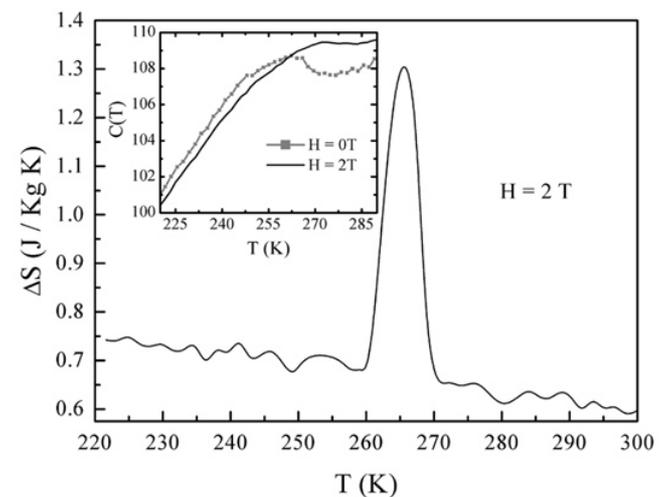

Figure 5. The magnetocaloric effect obtained from the heat capacity data. One can observe that the $|\Delta S|$ value near transition temperature is around 1.3 J/kg/K. The heat capacity for zero and 2 T field is shown in the inset.

netic materials close to T_C magnetic entropy decreases with increasing magnetic field and in an adiabatic condition that gives rise to an increase in temperature, positive ΔT_{ad}. The magnitude of ΔT_{ad} is maximum, where the rate of change of magnetization (as a function of temperature) is high. In order to calculate MCE from heat capacity data, the C/T versus T data in the temperature range 220–300 K, in presence of constant magnetic field, are integrated to find the temperature dependent entropy change ΔS_T using,

$$\Delta S_T(H) = \int_{T_{min}}^{T_{max}} \left(\frac{C(T,H)}{T} \right) dT. \qquad (3)$$

$|\Delta S|$ is then determined from $|\Delta S_{T,H=2T} - \Delta S_{T,H=0T}|$; the resulting data is plotted in figure 5, illustrating good agreement between the two methods. Further, we calculate the temperature change $|\Delta T_{ad}|$ realized by a change in magnetic field by using,

$$\Delta T_{ad} = -\int_0^{H_{max}} \left(\frac{T}{C(T,H)} \right) \left(\frac{\partial M}{\partial T} \right)_H dH. \qquad (4)$$

$C(T, H)$ in the above equation refers to the total heat capacity. A plot of $|\Delta T|$ versus T is shown in figure 4, and it exhibits a broad peak near the transition. The value $|\Delta T|$ was found to be 0·42 K at $T = 270$ K. Finally, we calculate the Relative Cooling Power (RCP),[9] which gives the cooling power of a refrigerator using the relations,

$$RCP(S) = |\Delta S_M|_{max} \times W(\Delta S_M), \qquad (5)$$

where, $W(\Delta S_M)$ denotes the full width at half maxima of magnetic entropy change curve. In the present case the RCP(S) is found to be 89 J kg^{-1}, which is comparable to those reported.

4. Conclusion

The magnitude of the magnetocaloric effect determined for $Pr_{0.1}Ce_{0.4}Sr_{0.5}MnO_3$ using magnetization and heat capacity data for a magnetic field change of 2 T is moderate ($\Delta S = 1·3$ J/K kg) compared to some of the manganese perovskite. However, the values of entropy change obtained from both methods are in good agreement. The relatively lower value of magnitude of the magnetocaloric effect may be due to incomplete structural transition near T_C.

References

1. Pecharsky V K and K A Gschneidner Jr 1997 *Phys. Rev. Lett.* **78** 4494
2. Rawat R and Das I 2006 *J. Phys.: Condens. Matter* **18** 1051
3. Giguere A, Foldeaki M, Ravi Gopal B, Chahine R, Bose T K, Frydman A and Barclay J A 1999 *Phys. Rev. Lett.* **83** 2262
4. Pecharsky V K, Tang H, Pecharsky A O, Schlagel D L, Lograsso T A and Gschneidner Jr K A 2003 *J. Appl. Phys.* **93** 8298
5. von Ranke P J, de Campos A, Caron A, Coelho A A, Gama S and de oliveira N A 2004a *Phys. Rev.* **B70** 94410
6. von Ranke P J, de Oliveira N A and Gama S 2004b *Phys. Lett.* **A320** 302
7. Chen P, Du Y W and Ni G 2000 *Europhys. Lett.* **52** 589
8. Neumeier J J, Hirotoshi Terashita and Garbe J J 2004 *Phys. Rev.* **B70** 94403
9. Dinesen A R, Linderoth S and Morup S 2005 *J. Phys.: Condens. Matter.* **17** 6257
10. Hong Zhu, Hao Song and YuHeng Zhang 2002 *Appl. Phys. Lett.* **81** 3416
11. Wolff Fabris F, Pekala M, Drozd V, Ru-Shi Liu, Ausloos M, J-F. Fagnard and Ph. Vanderbemden 2007 *J. Appl. Phys.* **101** 103904
12. Sande P, Hueso L E, Miguens D R, Rivas J, Rivadulla F and Lopez Quintela M A 2001 *Appl. Phys. Lett.* **79** 2040
13. Pecharsky V K, Gschneidner Jr K A and Tsokol A O 2005 *Rep. Prog. Phys.* **68** 1479
14. Sheng-Bo Tian, Manh-Huong Phan, Seong-Cho Yu and Nam Hwi Hur 2003 *Physica* **B327** 221
15. de Oliveira N A 2007 *Appl. Phys. Lett.* **90** 052501
16. Sundaresan A, Caignaert V, Maignan A, Suard E and Raveau B 1999 *Phys. Rev.* **B60** 533
17. Sundaresan A, Caignaert V, Raveau B and Suard E 1994 *Solid State Comm.* **104** 489
18. Anthony Arrott 1957 *Phys. Rev.* **108** 1394
19. Anthony Arrott and John E. Noakes 1967 *Phys. Rev. Lett.* **19** 786